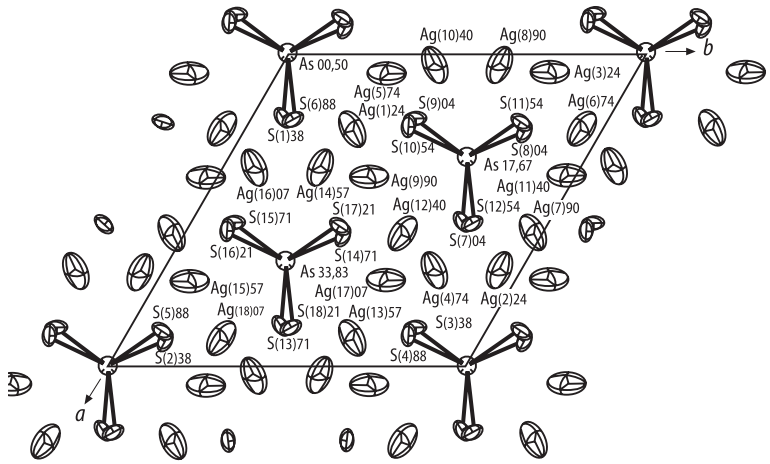

Fig. 23A-1-001. Ag_3AsS_3 (proustite). Crystal structure of phase I [85All]. Projection along the *c* axis. Atom labels are shown in parentheses, and the *c*-coordinates are given as a fraction [$\cdot 10^2$] of *c*. *T* = RT.

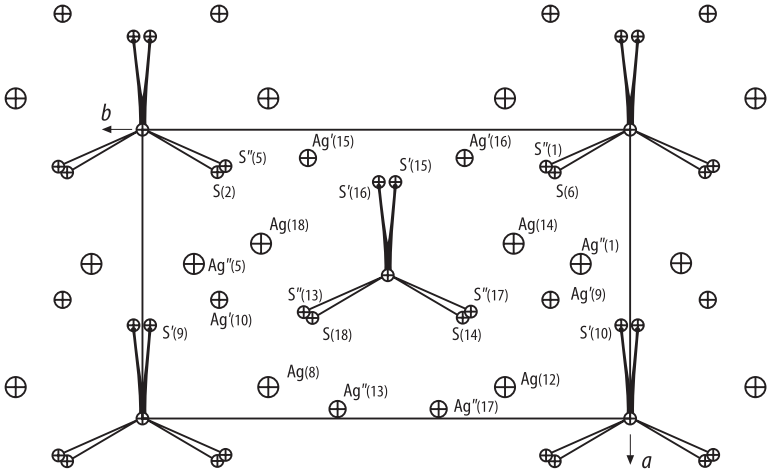

Fig. 23A-1-002. Ag_3AsS_3 (proustite). Crystal structure of phase IV [85All]. Projection along the *c* axis. The atoms are labeled with the number of the corresponding atom in Fig. 23A-1-001. The three independent sulfur atoms and silver atoms are labeled with S, S′, S″, and Ag, Ag′, Ag″, respectively.

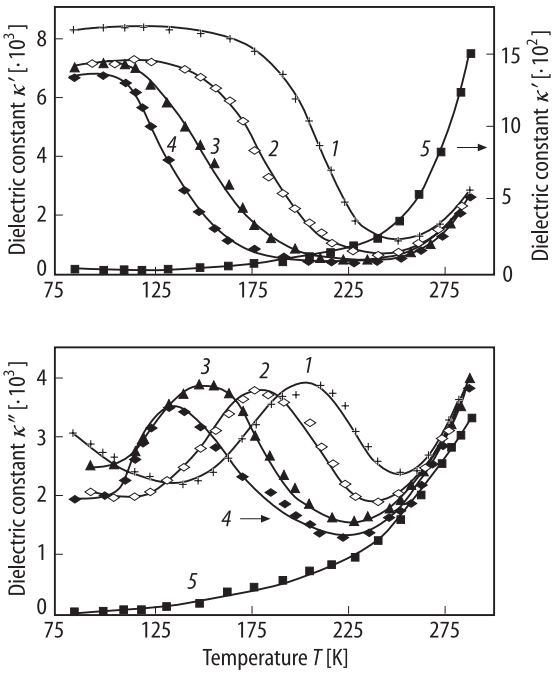

Fig. 23A-1-003. Ag_3AsS_3 (proustite). κ', κ'' vs. T [91Yan1]. Single crystal (measured axis is not indicated in the original paper). Parameter: W (light intensity from tungsten lamp). *1*: 1500 mW/cm^2, *2*: 500 mW/cm^2, *3*: 350 mW/cm^2, *4*: 50 mW/cm^2, *5*: dark. f = 1 kHz.

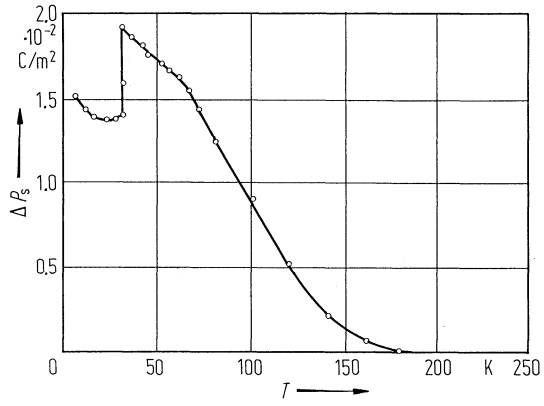

Fig. 23A-1-004. Ag_3AsS_3 (proustite). ΔP_s vs. T [75Nov]. ΔP_s: change of c component of the spontaneous polarization.

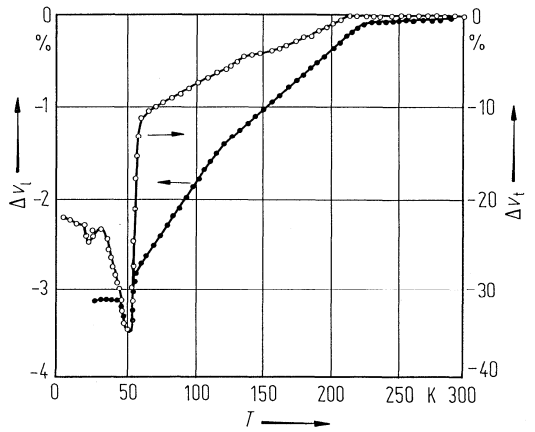

Fig. 23A-1-005. Ag_3AsS_3 (proustite). Δv_l, Δv_t vs. T [83Gor]. Δv_l, Δv_t: fractional change in the longitudinal and transverse sound velocities propagating along the c axis. f = 5 MHz. v_l = 2.7 km s^{-1}, v_t = 1.2 km s^{-1} at 300 K.

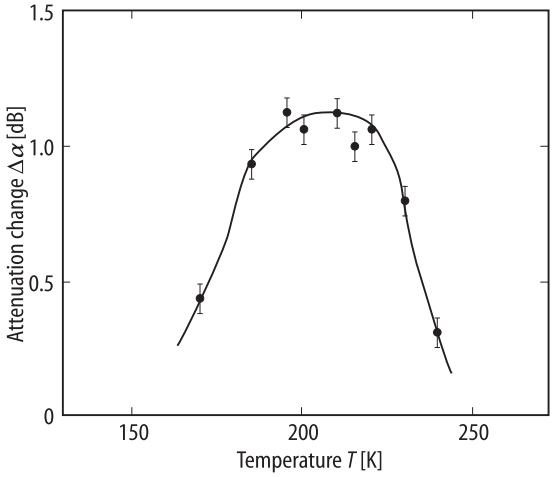

Fig. 23A-1-006. Ag_3AsS_3 (proustite). $\Delta\alpha$ vs. T [91Dun]. $\Delta\alpha$: change in the attenuation coefficient of the longitudinal sound (5.5 MHz) propagating along the c axis. The attenuation change is caused by the illumination of 2 mW light of a mercury lamp.

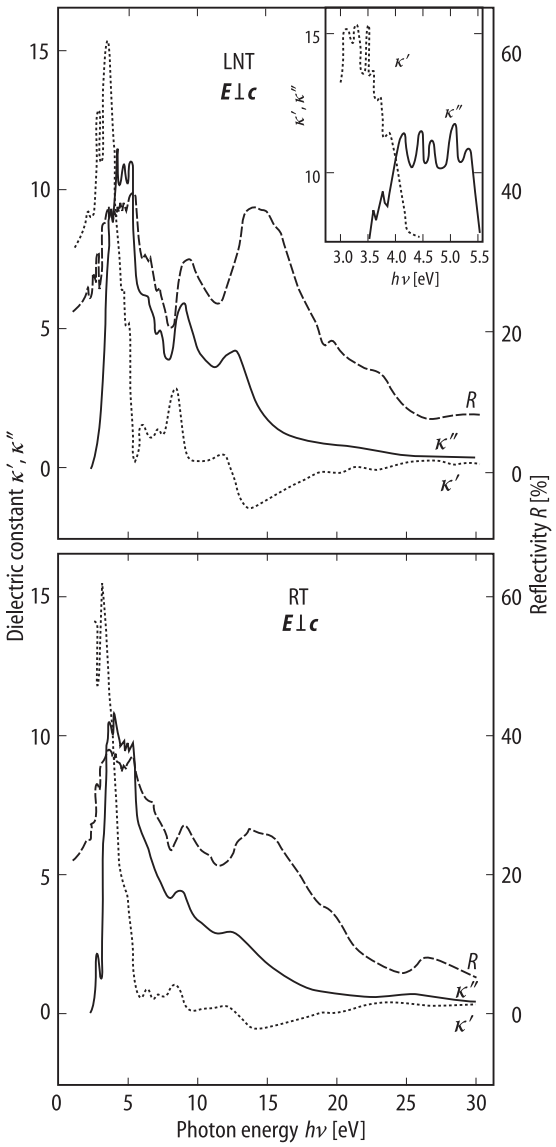

Fig. 23A-1-007. Ag_3AsS_3 (proustite). κ', κ'', R vs. $h\nu$ for polarization of light, $\boldsymbol{E} \perp \boldsymbol{c}$ at LNT (liquid nitrogen temperature) and RT [91Dov2]. R: reflectivity. κ' and κ'' were obtained from the reflectivity data using Kramers-Kronig relation.

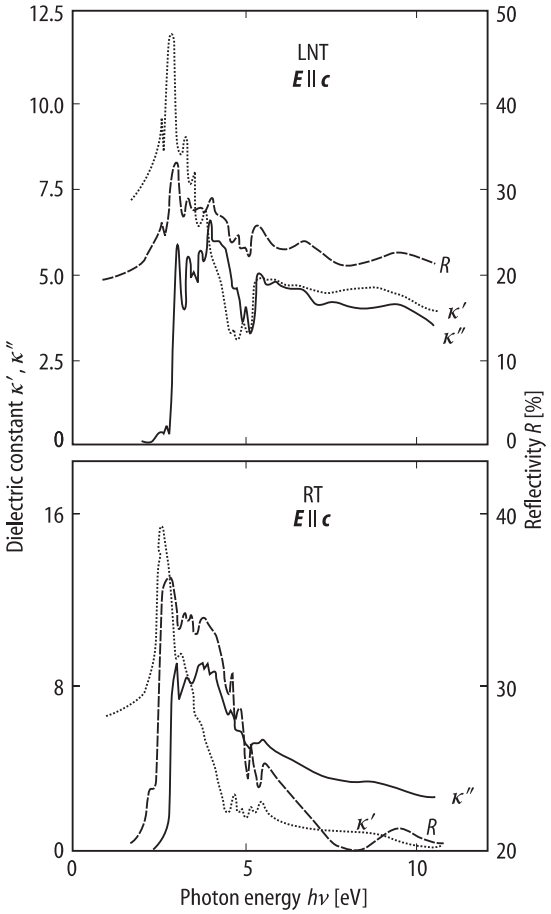

Fig. 23A-1-008. Ag_3AsS_3 (proustite). κ', κ'', R vs. $h\nu$ for polarization of light, $\boldsymbol{E} \parallel \boldsymbol{c}$ at LNT (liquid nitrogen temperature) and RT [91Dov2]. R: reflectivity. κ' and κ'' were obtained from the reflectivity by using Kramers-Kronig relation.

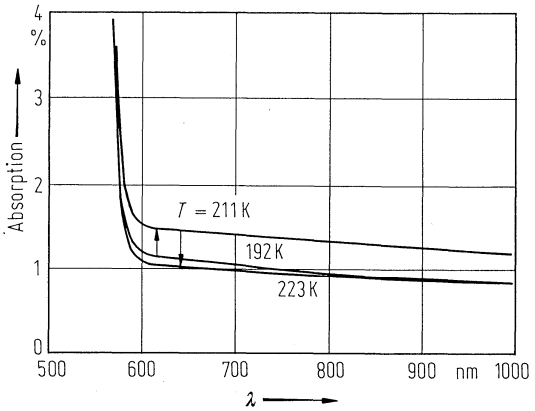

Fig. 23A-1-009. Ag_3AsS_3 (proustite). Optical absorption vs. λ for 4.6 mm thick sample [86Sha]. Parameter: T. Polarization of light, $\boldsymbol{E} \parallel \boldsymbol{c}$.

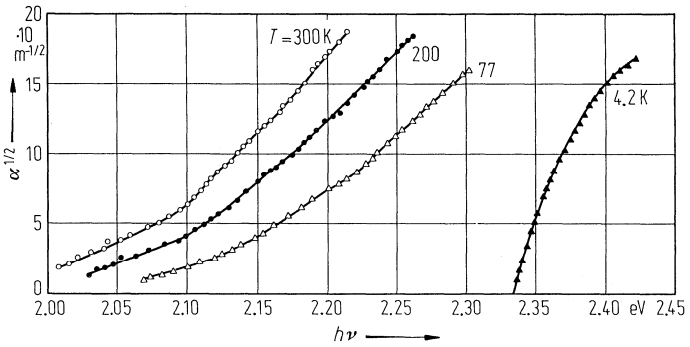

Fig. 23A-1-010. Ag_3AsS_3 (proustite). $\alpha^{1/2}$ vs. $h\nu$ near the absorption edge [71Dov]. Parameter: *T*. α: optical absorption coefficient. Polarization of light, $\boldsymbol{E} \parallel \boldsymbol{c}$.

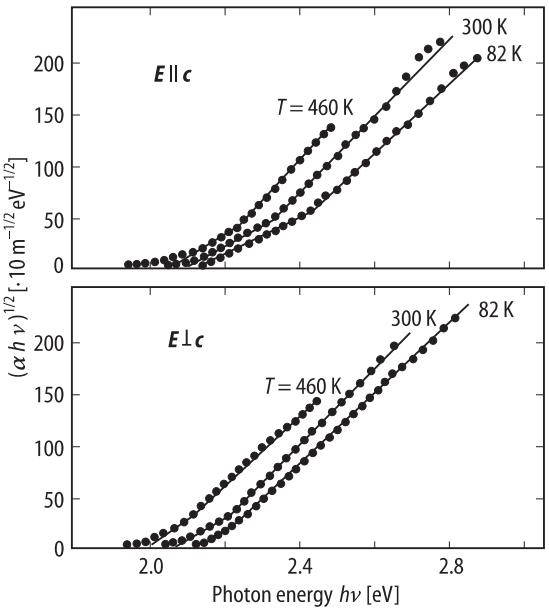

Fig. 23A-1-011. Ag_3AsS_3 (proustite). $(\alpha h\nu)^{1/2}$ vs. $h\nu$ [89Yan]. Parameter: *T*. α: optical absorption coefficient.

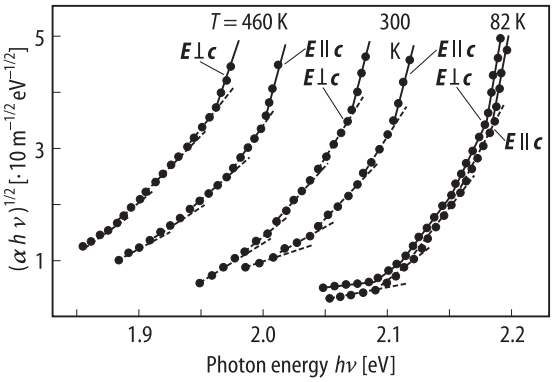

Fig. 23A-1-012. Ag_3AsS_3 (proustite). $(\alpha h\nu)^{1/2}$ vs. $h\nu$ [89Yan]. Parameter: *T*. α: optical absorption coefficient. Polarization of light, $\boldsymbol{E} \parallel \boldsymbol{c}$ or $\boldsymbol{E} \perp \boldsymbol{c}$.

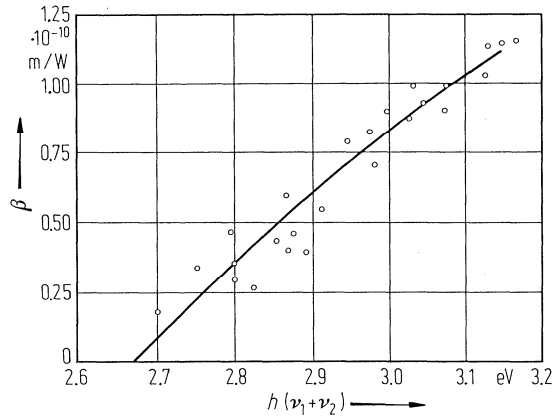

Fig. 23A-1-013. Ag_3AsS_3 (proustite). β vs. $h(\nu_1 + \nu_2)$ [75Ale]. β: two photon absorption coefficient. A two source method with neodymium laser beam was used.

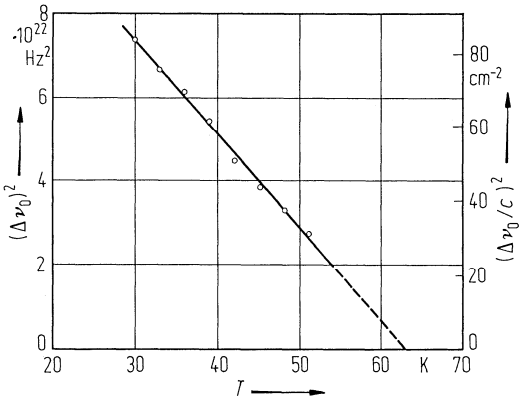

Fig. 23A-1-014. Ag_3AsS_3 (proustite). $(\Delta\nu_0)^2$ vs. T [83Ewe]. $\Delta\nu_0$: soft mode frequency measured by Raman spectroscopy.

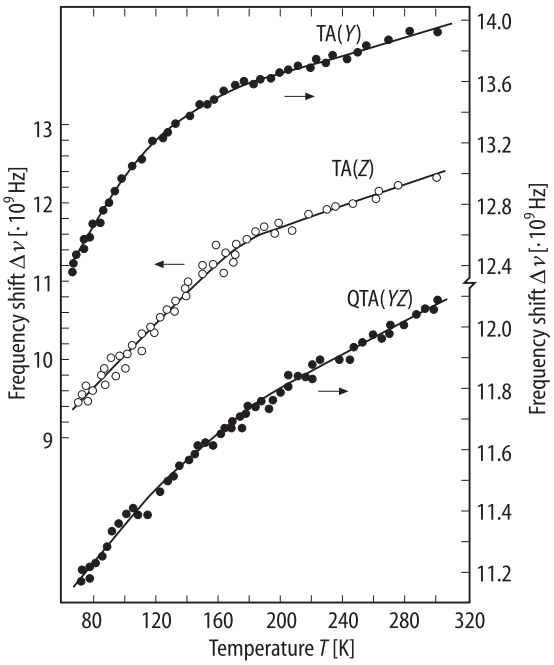

Fig. 23A-1-015. Ag_3AsS_3 (proustite). $\Delta\nu$ vs. T [81Smo]. $\Delta\nu$: Brillouin scattering frequency shift. TA(Y): transverse acoustic phonon traveling along the y axis in $Y(XZ)\overline{Y}$ scattering geometry, TA(Z): transverse acoustic phonon along the z axis in $Z(XX)\overline{Z}$ geometry, QTA(YZ): quasi-transverse acoustic phonon along the direction in the mirror symmetry plane at an angle 45° with respect to the y and z axes in $YZ(XX)\overline{YZ}$ geometry. λ = 647 nm.

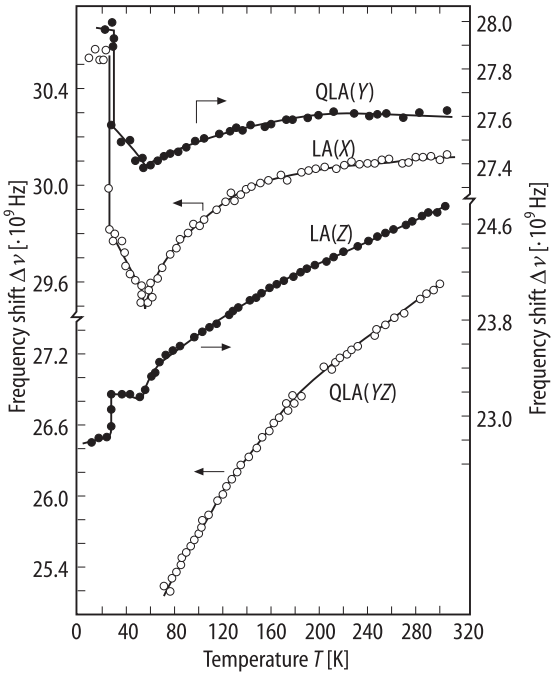

Fig. 23A-1-016. Ag_3AsS_3 (proustite). $\Delta\nu$ vs. T [81Smo]. $\Delta\nu$: Brillouin scattering frequency shift. QLA(Y): quasi-longitudinal acoustic phonon traveling along the y axis in $Y(XX)Y$ scattering geometry, LA(X): longitudinal acoustic phonon along the x axis in $X(YY)\overline{X}$ geometry, LA(Z): longitudinal acoustic phonon along the z axis in $Z(XX)\overline{Z}$ geometry, QLA(YZ): quasi-longitudinal acoustic phonon along the direction in the mirror symmetry plane at an angle 45° with respect to the y and z axes in $YZ(XX)\overline{YZ}$ geometry. λ = 647 nm.

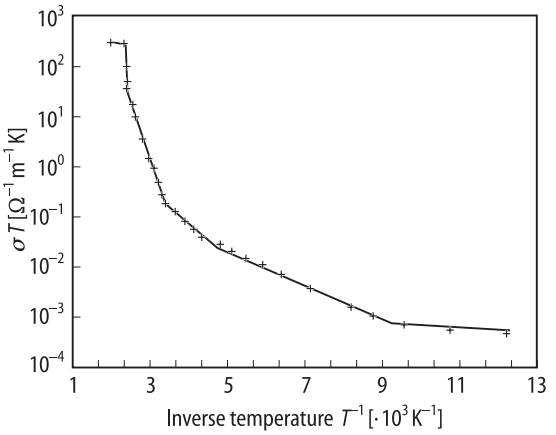

Fig. 23A-1-017. Ag_3AsS_3 (proustite). σT vs. T^{-1} [91Yan2]. σ: ac conductivity along the direction in the mirror symmetry plane, perpendicular to the trigonal axis. f = 1 kHz.

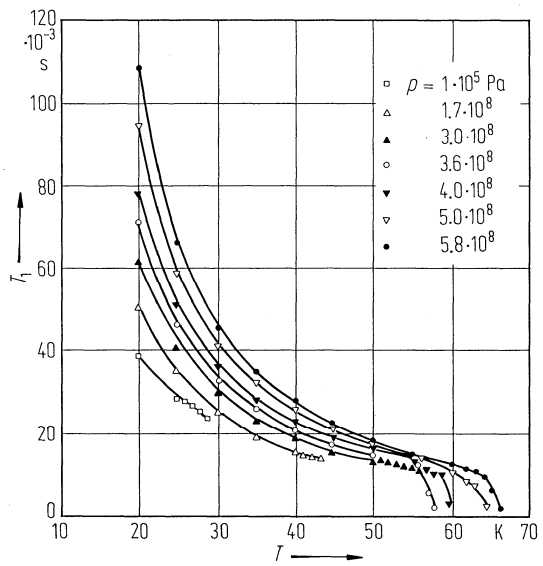

Fig. 23A-1-018. Ag_3AsS_3 (proustite). T_1 vs. T under hydrostatic pressure [82Bai]. Parameter: p. T_1: ^{75}As spin-lattice relaxation time.

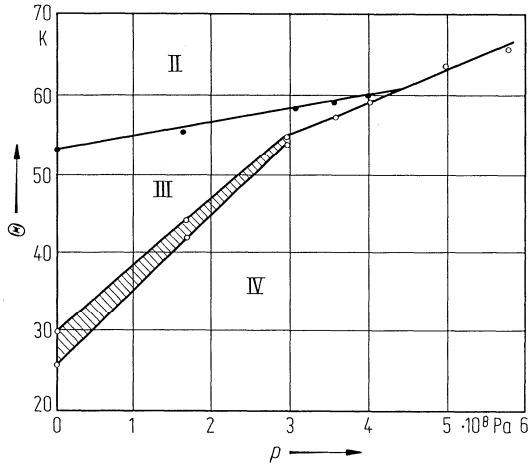

Fig. 23A-1-019. Ag_3AsS_3 (proustite). Θ–p phase diagram [82Bai]. ^{75}As NQR study. The region of temperature hysteresis is shaded.

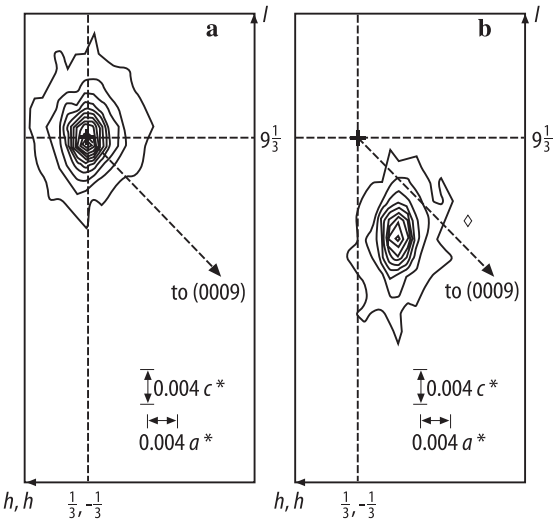

Fig. 23A-1-020. Ag_3AsS_3 (proustite). X-ray satellite scattering in phase II and III [85Rya]. Intensity distribution in the reciprocal space around (1/3, – 1/3, 0, 9 + 1/3). The curves show equi-intensity contours. The cross marks the commensurate position. (**a**) T = 45 K (phase III). (**b**) T = 51 K (phase II).

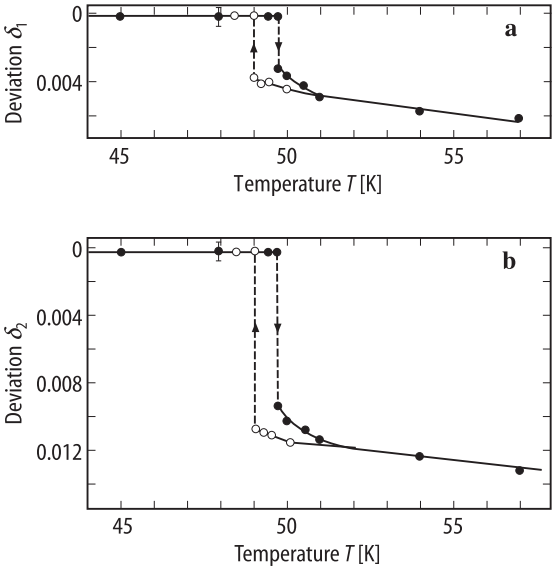

Fig. 23A-1-021. Ag_3AsS_3 (proustite). (**a**) δ_1 vs. T, (**b**) δ_2 vs. T [85Rya]. δ_1, δ_2: parameters which measure the deviation of the position of satellite reflection, (1/3 – δ_1, – (1/3 – δ_1), 0, 9 + 1/3 – δ_2), from the commensurate position (1/3, – 1/3, 0, 9 + 1/3).

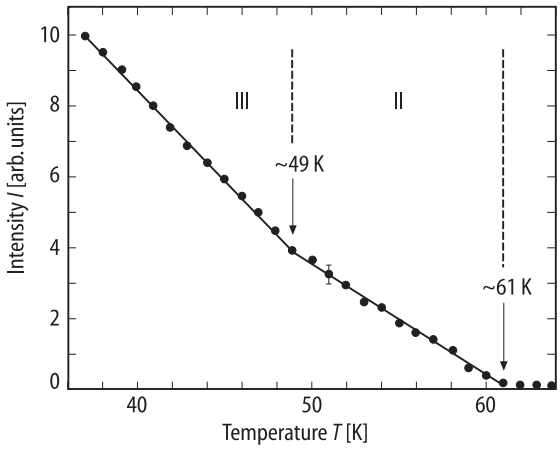

Fig. 23A-1-022. Ag_3AsS_3 (proustite). I vs. T [85Rya]. I: integrated intensity of X-ray reflection at $(1/3 - \delta_1, -(1/3 - \delta_1), 0, 9 + 1/3 - \delta_2)$ for $T > \Theta_{III-II}$ and at $(1/3, -1/3, 0, 9 + 1/3)$ for $T < \Theta_{III-II}$. For the meaning of δ_1 and δ_2, see the caption of Fig. 23A-1-021. The sample is cooled from 65 K at a rate of 4 K per hour.